



*Supplement of*

**Using a process-based dendroclimatic proxy system model in a data assimilation framework: a test case in the Southern Hemisphere over the past centuries**

**Jeanne Rezsöhazy et al.**

*Correspondence to:* Jeanne Rezsöhazy ([jeanne.rezsohazy@uclouvain.be](mailto:jeanne.rezsohazy@uclouvain.be))

The copyright of individual parts of the supplement might differ from the article licence.

## S1: Supplementary materials

**Table S1.** Pearson correlation coefficient between the observed tree-ring width (TRW) time series and the tree-ring index time series simulated by the regression model (Sect. 2.4.2) over 1950-2000 (calibration period) and 1901-1949 (verification period) at the 21 TRW sites of the PAGES2k databases (PAGES 2k Consortium, 2013, 2017). The site names are from the PAGES2k database: *Aus* for Tasmanian or New Zealand sites; *SAm* for South American sites. Asterisks stand for significant correlation coefficients at the 95% confidence level.

Site	Calibration	Verification
Aus_001	0.42*	-0.09
Aus_002	0.31*	-0.08
Aus_004	0.24	0.15
Aus_005	0.52*	-0.03
Aus_007	0.65*	0.35*
Aus_009	0.43*	-0.06
Aus_030	0.16	0.31*
Aus_031	0.25	-0.05
SAm_006	0.65	0.01
SAm_024	0.09	0.03
SAm_025	0.30*	0.50*
SAm_029	0.25	0.12
SAm_9	0.29*	-0.06
SAm_10	0.17	0.07
SAm_11	0.57*	0.22
SAm_12	0.31*	0.09
SAm_15	0.18	-0.04
SAm_16	0.18	0.21
SAm_17	0.20	0.22
SAm_18	0.09	-0.07
SAm_19	0.13	-0.15

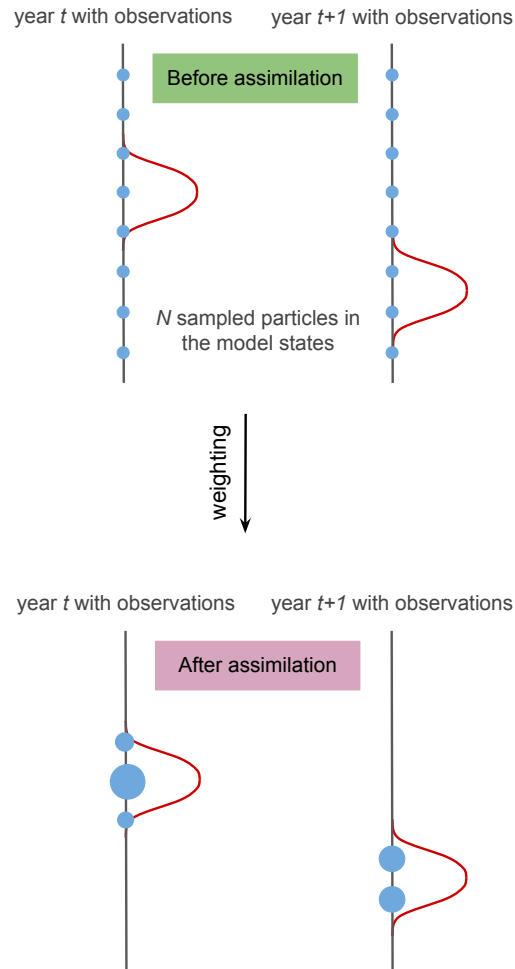


**Figure S1.** Before the assimilation, all the  $N$  ( $= 8$  in our example) particles (blue circles) sampled in the model states (vertical axis) have the same weight, which is proportional to the size of the circle, whatever the year considered ( $t$  and  $t+1$  in the example) because the prior is fixed throughout the assimilation procedure. The distribution of the available observations with uncertainties for each year is represented by the red curve. After the assimilation, the particles have been weighted relatively to their associated likelihood, given the available observations for each year, and the size of the circle is modified accordingly. When the weight of a particle is zero, it does not appear anymore on the figure. Figure and legend from Rezsöhazy (2021).

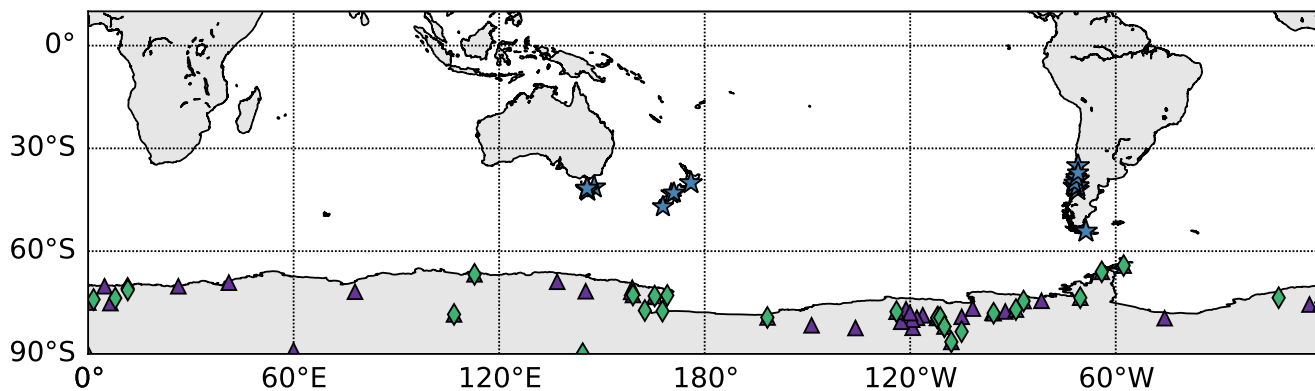


**Figure S2.** Location of the 21 tree-ring width (TRW) records (blue stars) from the PAGES2k databases (PAGES 2k Consortium, 2013, 2017); the 49 ice core snow accumulation records (purple triangles) from Thomas et al. (2017) and Medley et al. (2018); and the 29  $\delta^{18}O$  records (green diamonds) from Stenni et al. (2017) (Sect. 2.3). Background map from Hunter (2007).

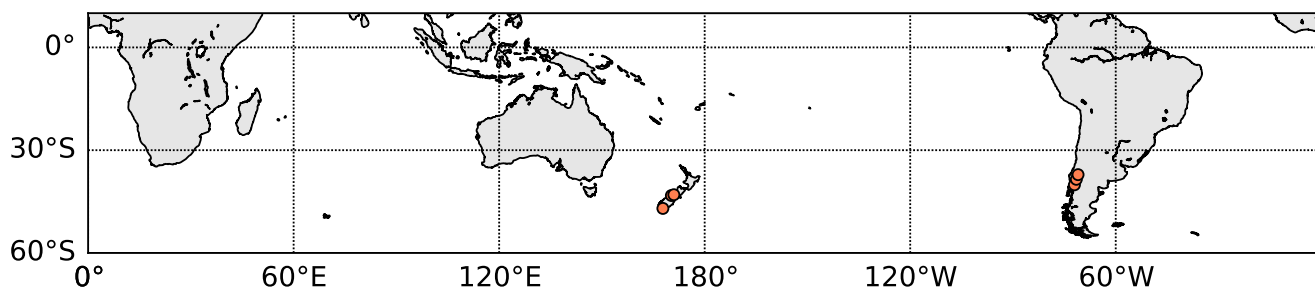


**Figure S3.** Location of the six tree-ring width (TRW) records (orange circles) from the PAGES2k databases (PAGES 2k Consortium, 2013, 2017) assimilated with the MAIDEN model calibrated over the 1950-2000 CE time period (see Sect. 2.4.1 for more details). Background map from Hunter (2007).

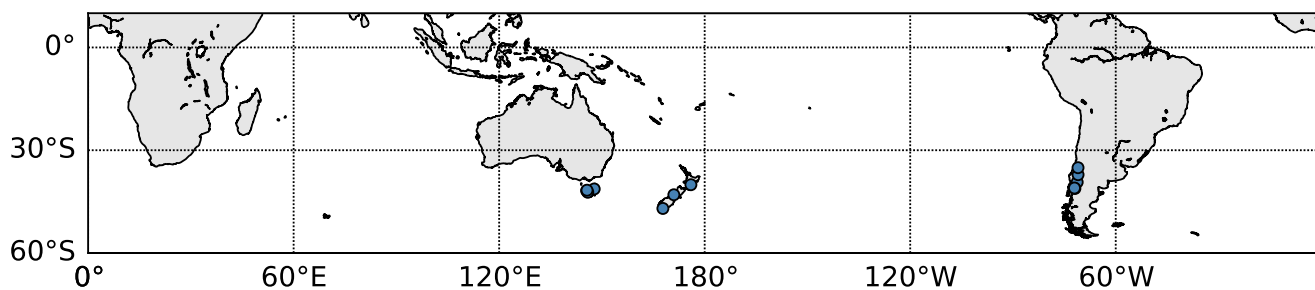


**Figure S4.** Location of the 12 tree-ring width (TRW) records (blue circles) from the PAGES2k databases (PAGES 2k Consortium, 2013, 2017) assimilated with the regression-based model calibrated over the 1901-2000 CE time period (see Sect. 2.4.2 for more details). Background map from Hunter (2007).

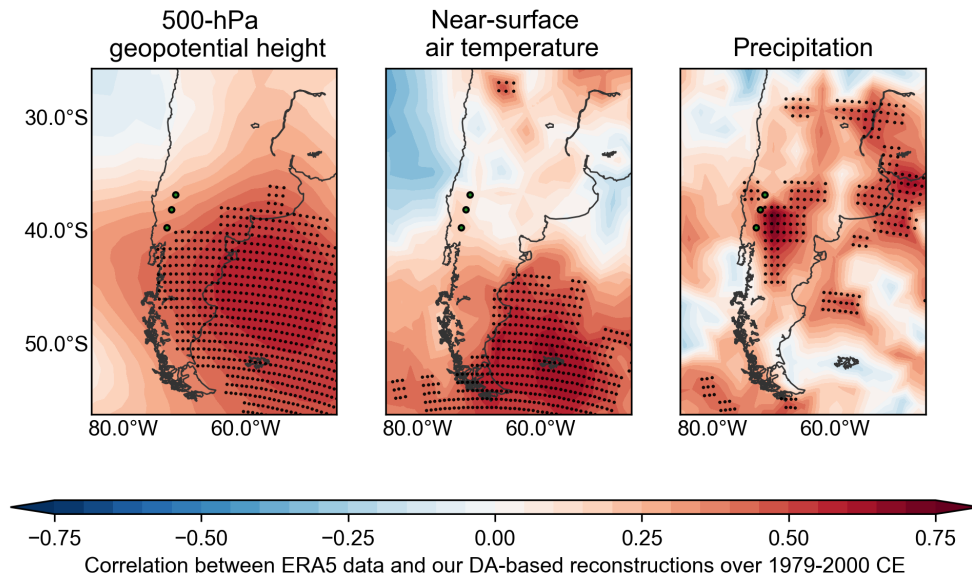


**Figure S5.** Pearson correlation coefficient between the reconstructed and ERA5 geopotential height at 500 hPa, near-surface air temperature or cumulative precipitation in South America over 1979-2000 CE for the TIC-MDN experiment (see Sect. 3 and Table 1 for details on the experiment). The green dots indicate the localization of the assimilated tree-ring width records. The black dots indicate a significant correlation coefficient at the 95% confidence level.

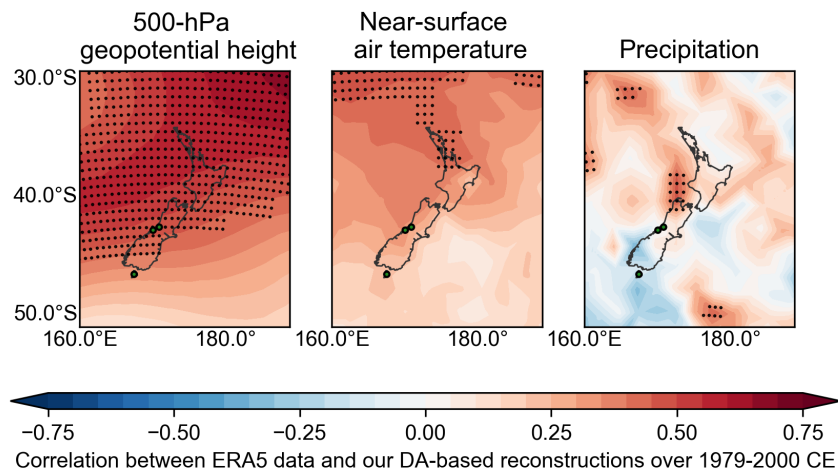


**Figure S6.** Pearson correlation coefficient between the reconstructed and ERA5 geopotential height at 500 hPa, near-surface air temperature or cumulative precipitation in New Zealand over 1979-2000 CE for the TIC-MDN experiment (see Sect. 3 and Table 1 for details on the experiment). The green dots indicate the localization of the assimilated tree-ring width records. The black dots indicate a significant correlation coefficient at the 95% confidence level.

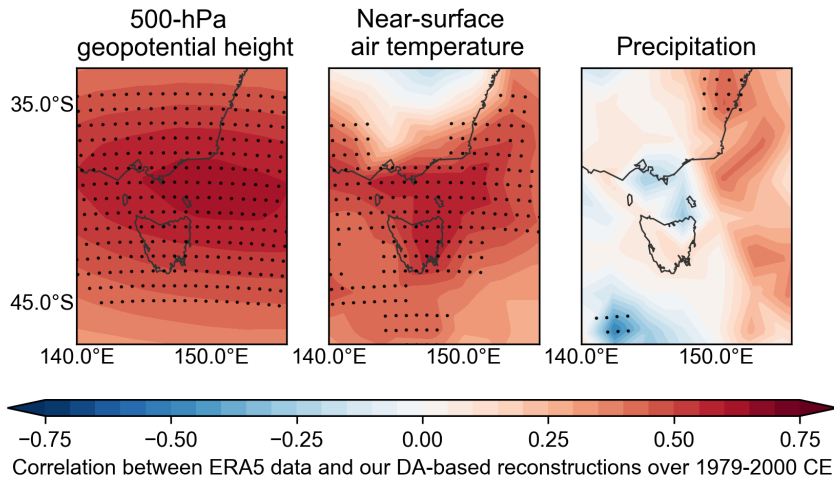


**Figure S7.** Pearson correlation coefficient between the reconstructed and ERA5 geopotential height at 500 hPa, near-surface air temperature or cumulative precipitation in Tasmania over 1979-2000 CE for the TIC-MDN experiment (see Sect. 3 and Table 1 for details on the experiment). The green dots indicate the localization of the assimilated tree-ring width records. The black dots indicate a significant correlation coefficient at the 95% confidence level.

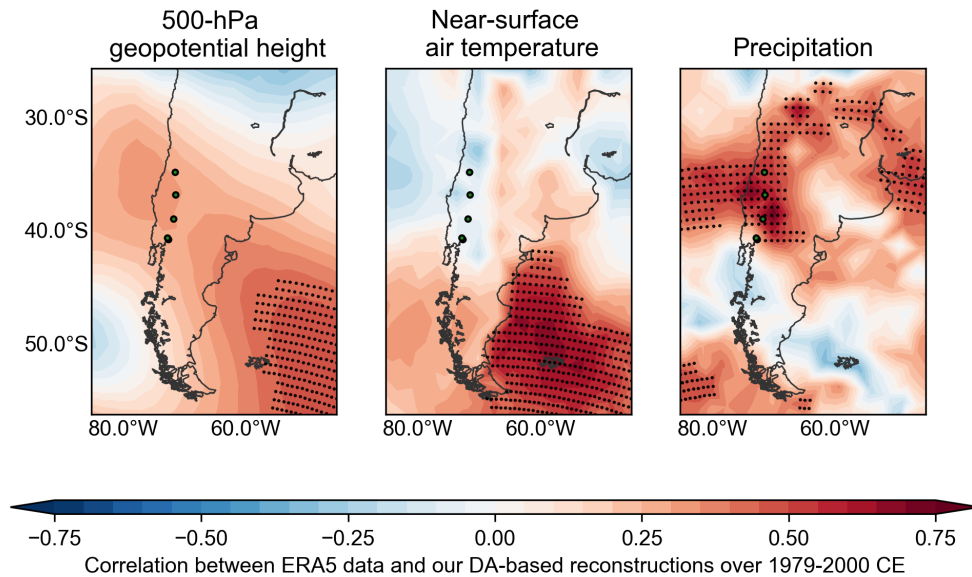


**Figure S8.** Pearson correlation coefficient between the reconstructed and ERA5 geopotential height at 500 hPa, near-surface air temperature or cumulative precipitation in South America over 1979-2000 CE for the TIC-reg experiment (see Sect. 3 and Table 1 for details on the experiment). The green dots indicate the localization of the assimilated tree-ring width records. The black dots indicate a significant correlation coefficient at the 95% confidence level.

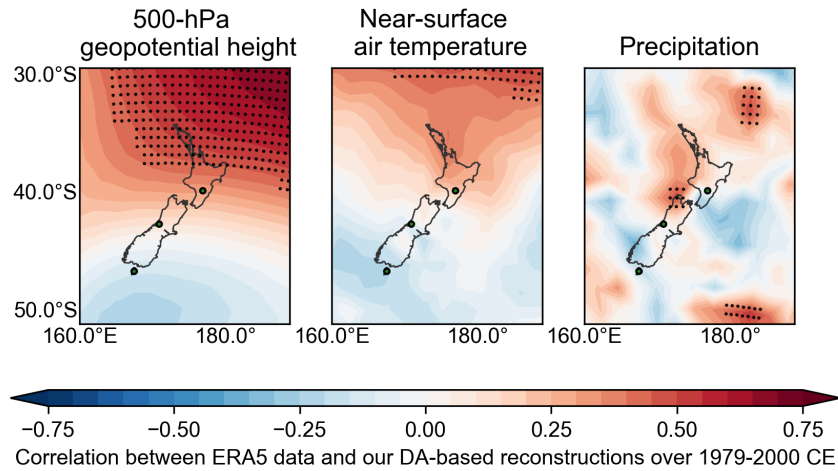


**Figure S9.** Pearson correlation coefficient between the reconstructed and ERA5 geopotential height at 500 hPa, near-surface air temperature or cumulative precipitation in New Zealand over 1979-2000 CE for the TIC-reg experiment (see Sect. 3 and Table 1 for details on the experiment). The green dots indicate the localization of the assimilated tree-ring width records. The black dots indicate a significant correlation coefficient at the 95% confidence level.

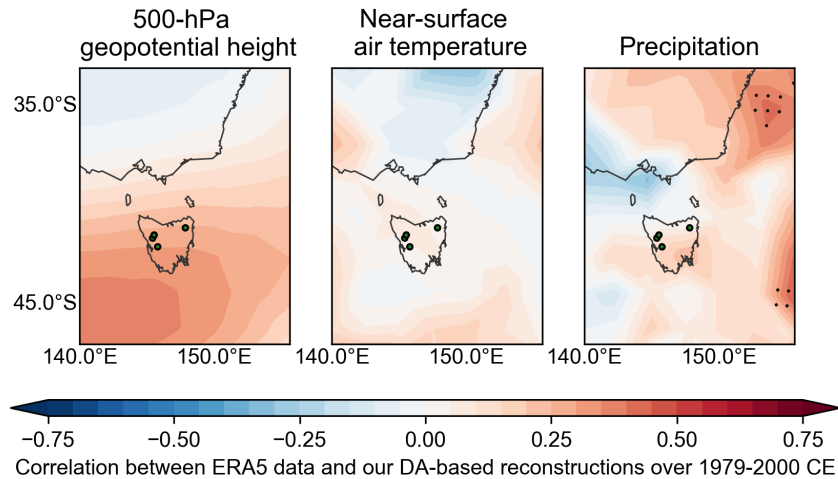


**Figure S10.** Pearson correlation coefficient between the reconstructed and ERA5 geopotential height at 500 hPa, near-surface air temperature or cumulative precipitation in Tasmania over 1979-2000 CE for the TIC-reg experiment (see Sect. 3 and Table 1 for details on the experiment). The green dots indicate the localization of the assimilated tree-ring width records. The black dots indicate a significant correlation coefficient at the 95% confidence level.

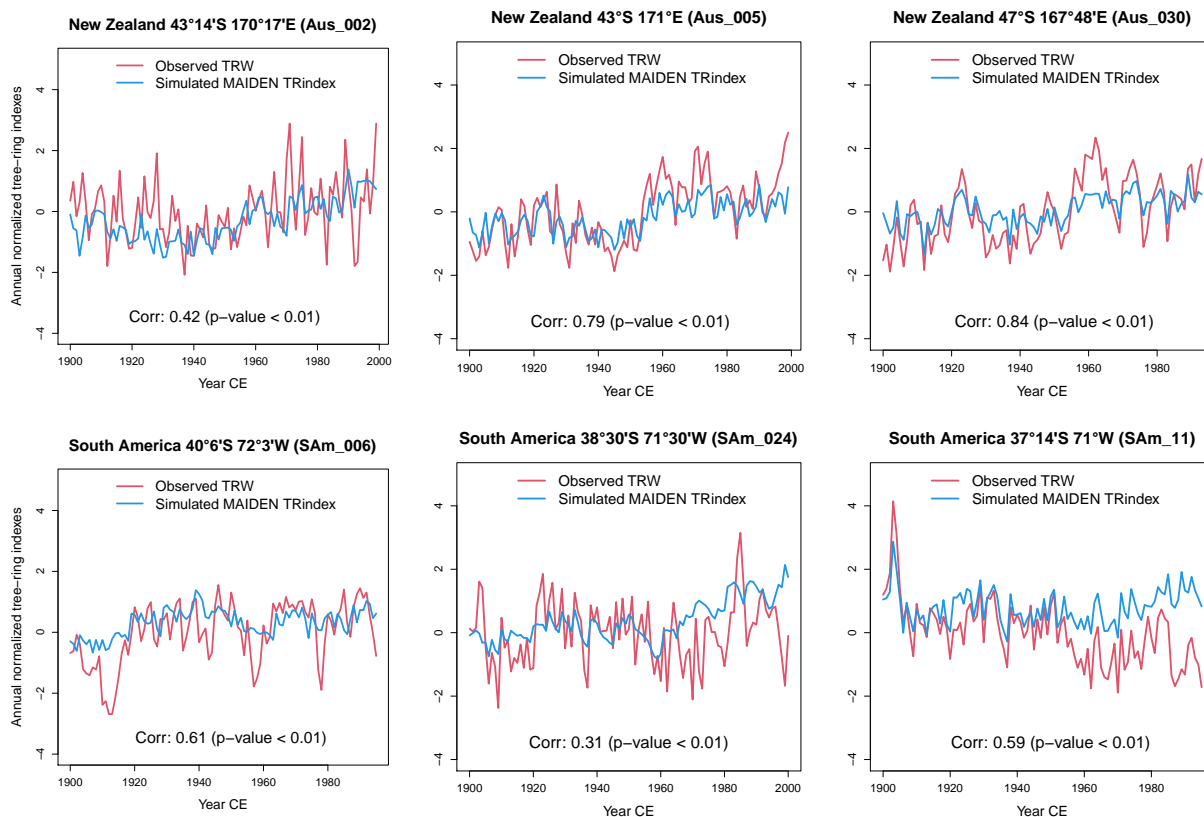


**Figure S11.** Observed tree-ring width and simulated tree-ring index by MAIDEN over 1900-2000 CE at the six assimilated tree-ring width sites (Sect. 2.4.1). Pearson correlation coefficient (Corr) between observed and simulated tree-ring index and associated p-value. The observations are normalized relative to 1900-2000 CE. The simulations are normalized relative to 1900-2000 CE using the mean and the standard deviation of the reference run of MAIDEN with the iCESM1 data used in the data assimilation procedure (Sect. 2.4.1). The TIC-MDN reanalysis is used to run MAIDEN (see Sect. 3 for details on the data assimilation experiment).

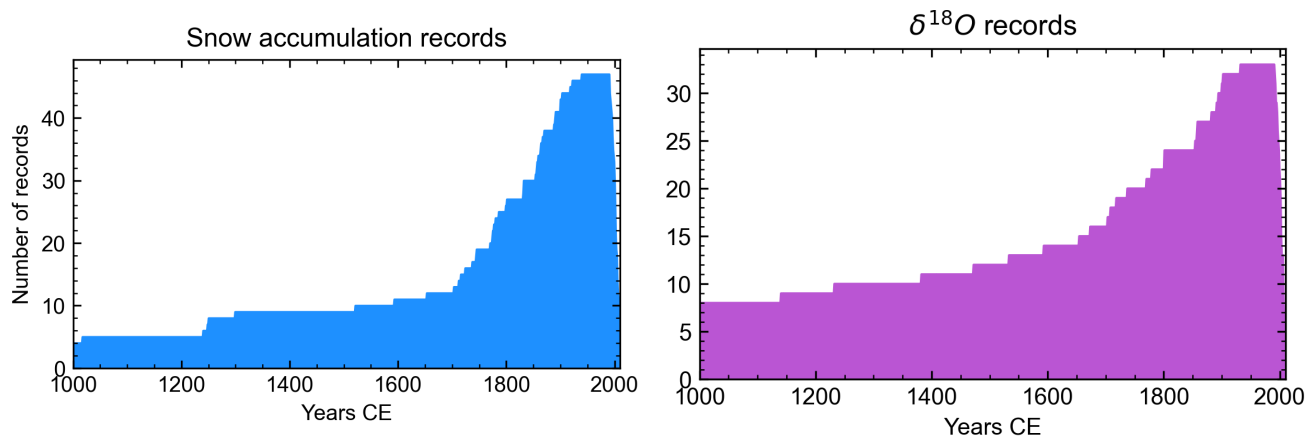


**Figure S12.** Number of snow accumulation and  $\delta^{18}\text{O}$  records used in this study (Sect. 2.3.2) over 1000-2000 CE. Figures from Dalaiden et al. (2021).

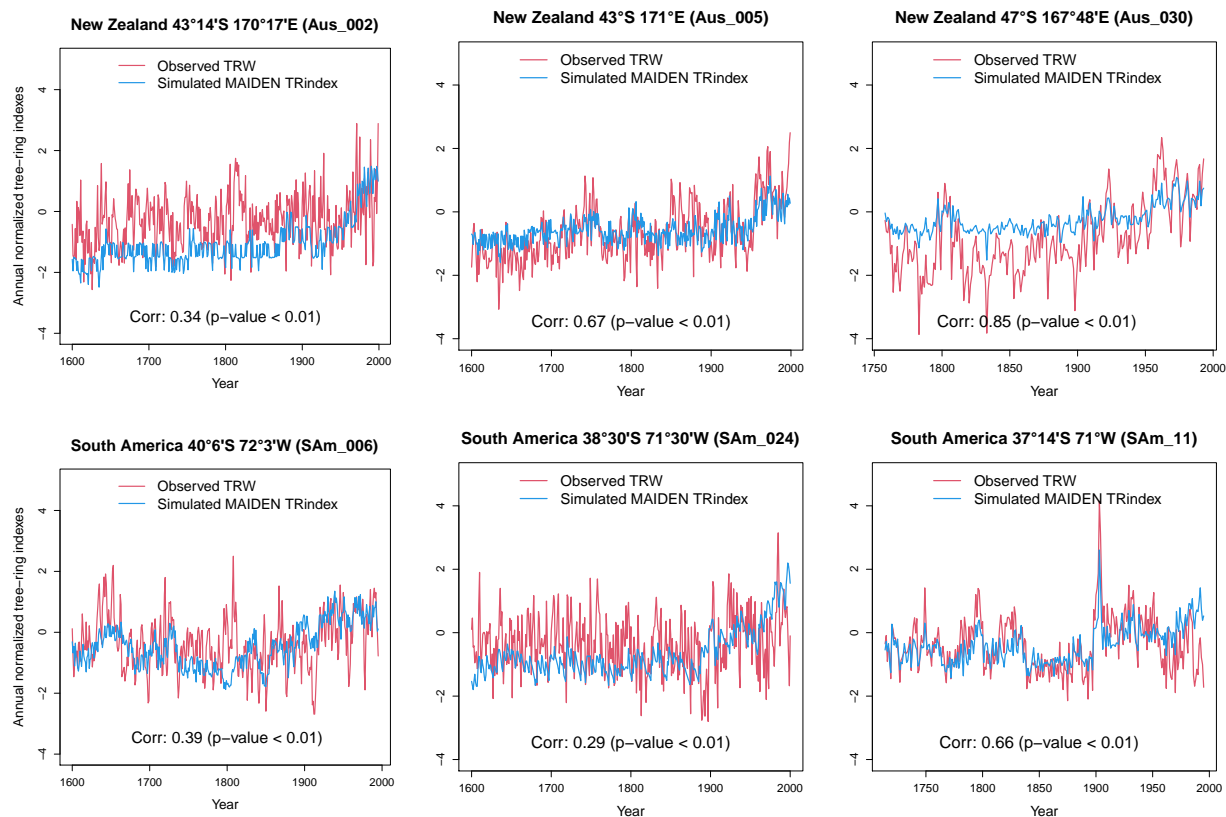


**Figure S13.** Observed tree-ring width and simulated tree-ring index by MAIDEN over 1600-2000 CE at the six assimilated tree-ring width sites (Sect. 2.4.1). Pearson correlation coefficient (Corr) between observed and simulated tree-ring index and associated p-value. The observations are normalized relative to 1900-2000 CE. The simulations are normalized relative to 1900-2000 CE using the mean and the standard deviation of the reference run of MAIDEN with the iCESM1 data used in the data assimilation procedure (Sect. 2.4.1). The TIC-MDN reanalysis is used to run MAIDEN (see Sect. 3 for details on the data assimilation experiment).